ANALYSIS OF ELASTOMERIC PAVEMENT SEALS

Ravindra K. Vyas, University of Utah, Salt Lake City

The objective of this paper is to present a method for predicting the load deflection characteristic and maximum stresses in elastomeric seals. The basic problem is reduced to the structural analysis of V-shaped web members for large flexural deformations. The analysis is presented in terms of dimensionless quantities, with sample results in tabular and graphical form. The dimensionless results are used to construct the predicted load deflection curve for an actual sample and to compare it with the experimental load deflection curve for the same sample. The values of elastic moduli necessary for constructing the curve were obtained by laboratory experiments. Results indicate that a successful prediction of load deflection behavior and maximum stresses can be made theoretically. The prediction gives a good estimate of load deflection behavior up to 60 percent deformation; beyond this value the sample ceases to respond as a structure and becomes more like a mass of neoprene. The predicted maximum stresses for a particular example are given in graphical form. The results show that maximum shear stress is very low, so that shear deformations may be neglected; the tensile and compressive stresses, however, do have significant values.

•THE ELASTOMER polychloroprene, more commonly known as neoprene synthetic rubber, is a product suited to a variety of uses. Various types of neoprene, with different compositions and properties, are commercially available. Neoprene is an important chemical component of most of the elastomeric pavement seals available today.

The problem of effectively sealing concrete pavement joints is perhaps as old as the concrete pavement itself. To the designer it presents a complex problem because of the many variables that must be taken into account. Tons (1) and Cook (2, 3) have dealt with some important aspects of the joint design problem. Neoprene seals combine flexibility with resilience, 2 prime factors necessary for satisfactory performance of any pavement joint seal. This fact perhaps explains the encouraging findings of Hiss et al. (4) as well as the gain in popularity of elastomeric seals in recent years.

Neoprene seals for pavement joints are available in long coils of tubelike structures with varying section geometry. The interior of the tube is strengthened by means of a gridwork of thin flexible members. Figure 1 shows one such seal section in detail. The manufacturers of elastomeric seals have been constantly experimenting with the chemical composition and also with the section geometry in order to improve the product. The performance of these seals is currently being studied by a group of research and academic institutions. This paper contains a portion of such an investigation in progress under the direction of the author at the University of Utah.

An important criterion in assessing the performance of a neoprene seal is its load deflection characteristic. The load deflection curve of a given sample can be obtained experimentally. However, it is desirable to develop the analytical technique for predicting this characteristic before the product is manufactured. The main objective of this paper is to present such a technique. In order to make the results more useful, the analysis is carried out in general terms; dimensionless forces and dimensionless displacements are used. Sample results of the theoretical study are presented in tab-

Sponsored by Committee on Sealants and Fillers for Joints and Cracks and presented at the 50th Annual Meeting.

ular and graphical form. From the dimensionless results the theoretical load deflection curve for the section shown in Figure 1 is plotted by using the actual values of the elastic moduli and the geometric parameters α, t, and ℓ. The results of experiments on the same sample are also plotted for the purpose of comparison. An advantage of the analytical technique is that it enables the designer to evaluate the maximum stresses.

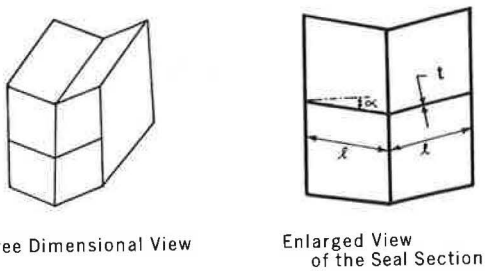

Three Dimensional View — Enlarged View of the Seal Section

Figure 1. A neoprene pavement seal.

The physics and chemistry of rubber and rubberlike materials are adequately described in standard works (5, 6, 7). Our experimental work indicates, as would be expected, that neoprene is a viscoelastic solid. The stress-strain behavior of the material can most probably be simulated by a Kelvin chain (8). The simplest possible model of this type would, of course, be the 3-parameter solid. The viscoelastic character of the material complicates the task of the analysis. However, the experiments also indicate that, for short durations of time, the stress-strain behavior of the material can be treated as time-independent.

In order to make it as simple as possible, this presentation of the initial attempt is restricted to the short time load deflection characteristic. It is assumed that, in the range of deformations of interest, the strain is small enough so that the stress-strain curves for the material in tension and compression can be treated as reasonably linear. The corresponding values of the elastic moduli of the material in tension and in compression have to be obtained from laboratory experiments. Such experiments were conducted by the Utah State Department of Highways to determine these moduli for the material of some samples. These experiments were performed at room temperature, with adequate repetitions to ensure reliability, on flat strips cut out from actual samples. The results of these efforts are given in Table 1. The material properties vary considerably, which is not surprising in view of the empirical efforts to improve the product and the fact that the material properties are also affected by the process of extrusion and subsequent curing.

An advantage of the analytical approach in general terms is that one need not worry about these variations in material properties at the outset. The values of elastic moduli are needed only when one wants to predict the behavior of a given sample. For research purposes these values can be obtained from laboratory experiments; for design purpose it would be desirable to have these values furnished by the manufacturers as a matter of course.

TABLE 1

SAMPLE VALUES OF MODULI OF ELASTICITY AT ROOM TEMPERATURE

Material	E_T(psi)	E_C(psi)	E_T/E_C
A	808	531	1.522
B	603	780	0.773
C	717	903	0.794

Note: E_C = modulus of elasticity in compression; and E_T = modulus of elasticity in tension.

ANALYSIS

Any analysis, to be of value to the practical engineer, has to be as simple as possible. An effort has been made in this paper to concentrate on the essentials of the problem and to focus the attention on important patterns. An inevitable consequence of such an effort is the simplifying assumptions necessary in the process. Two simplifying assumptions have already been stated in the introductory remarks: (a) only short-time load deflection response is considered, and (b) the strains are small enough to justify a linear stress-strain relationship. It must be noted, however, that small strain does not imply small deformations; indeed, the problem being investigated involves large deformations.

In addition to these assumptions, the present analysis is confined to seal sections that have a specific geometric pattern. The sec-

tion shown in Figure 1 gives one of the typical patterns in its simplest form. Basically the pattern may be described as a symmetrical system of 2 vertical side walls and an internal vertical diaphragm. In addition, there are a series of V-shaped members, called web members, joining the side walls and intersecting the diaphragm. All the web members are assumed to be identical and of constant thickness. During load deflection experiments, the vertical side walls are forced to move toward each other while remaining mutually parallel. The side walls are at all times vertical and straight. The resistance to displacement, then, is derived from the web members. Two of the following assumptions are based on the preceding discussion:

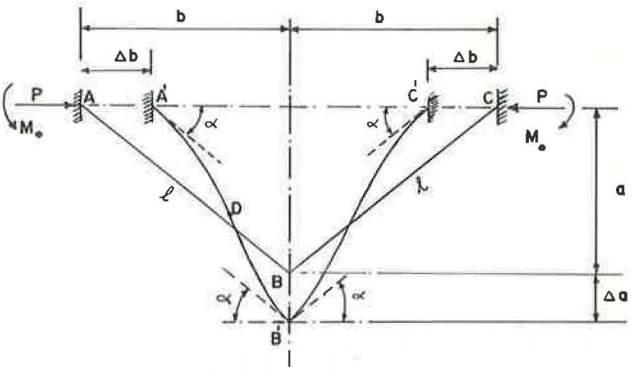

Figure 2. V-shaped web member.

1. The seal section is perfectly symmetrical about the central diaphragm;
2. The resistance to deformation is proved entirely by the web members, and all the web members are assumed to be identical and of constant thickness; and
3. In addition, it is assumed that the deformations are produced by bending only (the effects of axial compression and shear are treated as negligible in the present analysis).

With these assumptions, the task of analysis reduces to the study of flexural deformations of the typical configuration shown in Figure 2. When subjected to a load P, the system deforms into the configuration A′ B′ C′ shown in this figure. Corresponding to a given end load P, a correct end moment M_0 must be applied as shown to provide complete restraint against end rotation. The object of the analysis is to find the deflections Δa and Δb, the end moment M_0, and the maximum stresses for a given load P.

Because of symmetry, it is sufficient to restrict our attention only to the left member AB. Also because of symmetry, the point of zero curvature is located at a point D midway along the length AB. The entire problem, then, may be solved by confining the analysis to the length AD (Fig. 3).

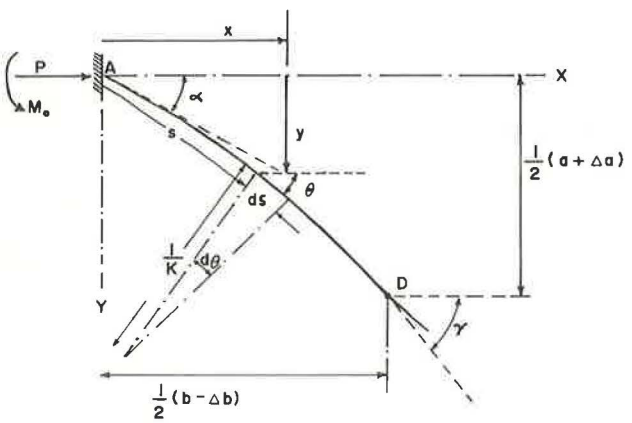

Figure 3. Kinematics of deformation.

The moment curvature relationship for large flexural deformations of this member is given by

$$M(s) = -EIK(s) \qquad (1)$$

where

M(s) = bending moment at s;
E = reference elastic constant (either E_C or E_T);
I = geometric constant (modified moment of inertia corresponding to the chosen elastic constant E); and
K(s) = curvature at s.

From geometry, kinematics of deformation, and equilibrium respectively, we have

$$dx = ds \cos \theta, \text{ and } dy = ds \sin \theta \tag{2}$$

$$K(s) = d\theta/ds \tag{3}$$

$$M(s) = Py - M_o \tag{4}$$

Substitution from Eq. 3 and 4 into 1 and then differentiation with respect to s yields

$$(d^2\theta/ds^2) + k^2 \sin \theta = 0 \tag{5}$$

where

$$k^2 = P/EI \tag{6}$$

Finally integrating Eq. 5 with respect to s and imposing the condition that as $s = 0$, $\theta = \alpha$, and $d\theta/ds = -(M_o/EI)$, we obtain

$$d\theta/ds = \sqrt{(M_o/EI)^2 - 2k^2 \cos \alpha + 2k^2 \cos \theta};\ 0 \le s \le \ell/2 \tag{7}$$

From Eq. 7, the angle γ at inflection point is obtained as

$$\cos \gamma = \cos \alpha - (M_o/EI)^2 (1/2k^2) \tag{8}$$

Also from Eq. 7, we obtain

$$\int_0^{\ell/2} ds = \int_\alpha^\gamma \frac{d\theta}{\sqrt{(M_o/EI)^2 - 2k^2 \cos \alpha + 2k^2 \cos \theta}} \tag{9}$$

Next, the following dimensionless quantities are introduced:

$$u = k\ell = \sqrt{P/EI}\ \ell \tag{10}$$

$$v = M_o \ell/EI \tag{11}$$

$$\Delta = \Delta b/b \tag{12}$$

$$\Delta' = \Delta a/a \tag{13}$$

In Eqs. 10 through 13, u and v are dimensionless force and dimensionless end moment respectively; and Δ and Δ' are dimensionless horizontal and vertical deformations respectively. The discussion that follows will be in terms of these dimensionless quantities. Next, let

$$p = \sin \gamma/2 \tag{14}$$

and

$$p \sin \phi = \sin \theta/2 \tag{15}$$

then, integrating Eq. 9 and using Eqs. 8 through 13, we obtain

$$u = 2 \int_{\phi_o}^{\pi/2} \frac{d\phi}{\sqrt{1 - p^2 \sin^2 \phi}} \tag{16}$$

where

$$\phi_o = \sin^{-1} [(\sin \alpha/2)/(\sin \gamma/2)] \tag{17}$$

In terms of the dimensionless quantities, the angle γ is expressed by

$$\gamma = \cos^{-1} [\cos \alpha - (v^2/2u^2)] \tag{18}$$

The displacements of any point of the member ABC can be obtained by integrating Eq. 2 and using symmetry principle. The quantities of interest here are the deformations Δ and Δ'. Of these, Δ can be obtained by integrating the first of Eq. 2, and Δ' can be obtained from the requirement of zero bending moment at the point of inflexion. The final expressions for Δ and Δ' are as follows:

$$\Delta = [1 + (1/\cos \alpha)] - (4/u \cos \alpha) \int_{\phi_o}^{\pi/2} \sqrt{1 - p^2 \sin^2 \Phi}\, d\Phi \tag{19}$$

$$\Delta' = [2v/(u^2 \sin \alpha)] - 1 \tag{20}$$

Equations (1 through 20 present briefly the essential points of the analysis. It is basically a variation of the well-known problem of elastica, first investigated by Euler. Euler's elastica, which refers to the large flexural deformations of a thin straight elastic rod, is described in sufficient detail in standard sources (9, 10). The present problem differs from Euler's elastica in that it deals with the large flexural deformations of a V-shaped rod. Hence, trigonometric functions of the characteristic configuration angle α appear in the preceding expressions. The load deformation curves are much influenced by this angle.

The integrals in Eqs. 16 and 19 are incomplete elliptic integrals of the first and second kind (11). Hence, it is necessary to use numerical integration procedures to evaluate the required quantities. From Eqs. 17 through 20, it can be seen that for a given u we can evaluate all the quantities, provided we know the value of either the end moment v or the angle γ at the inflection point. It is sufficient to know only one of these 2 quantities. Therefore, the problem can be looked on as statically or kinematically indeterminate to the first degree, depending on whether v or γ is treated as the unknown quantity. It can be seen that the integral in Eq. 16 will be equal to the given value of u only for the correct choice of v or γ. The correct values of either of these quantities have to be obtained by the process of numerical interpolation. This discussion, of course, applies only to the case where one wants to solve the problem for a specific value of u. The task of constructing the theoretical load deflection curve is numerically much easier. This is done by using the kinematic method, which relies on finding u for progressively increasing values of γ.

TABLE 2

SAMPLE COMPUTATIONS FOR A CONFIGURATION ANGLE α = 8.5 DEG

γ (deg)	u^2 (= PL^2/EI)	v (= M_oL/EI)	Δ (percent)	Δ' (percent)
9.5	0.8611	0.0686	0.1813	0.0775
11.5	2.1981	0.1999	0.5888	0.2306
15.5	3.965	0.4487	1.5834	0.5311
19.5	5.0975	0.6876	2.8156	0.8252
22.5	5.7221	0.8634	3.8940	1.0416
27.5	6.5161	1.1530	5.9805	1.3942
32.5	7.1256	1.4406	8.4200	1.7356
37.5	7.6292	1.7279	11.2015	2.0645
42.5	8.0708	2.0158	14.31	2.379
47.5	8.4776	2.305	17.73	2.679
52.5	8.8674	2.5969	21.46	2.962
57.5	9.25[illegible]	2.8913	25.47	3.228
67.5	10.04	3.491	34.26	3.700
77.5	10.93	4.1097	43.95	4.087
87.5	11.95	4.753	54.37	4.381
97.5	13.17	5.431	65.35	4.578
107.5	14.68	6.154	76.71	4.671
110.5	15.20	6.328	80.17	4.678

The kinematic method can be briefly described as follows: As the load u is increased from zero, the system deforms progressively, and the angle γ at the inflection point increases as u increases. Hence, it is only necessary to select progressively increasing values of γ ($> \alpha$) in suitable increments and to evaluate the corresponding values of u, v, Δ, and Δ'. The numerical work is easily done with the digital computer, and the process is ter-

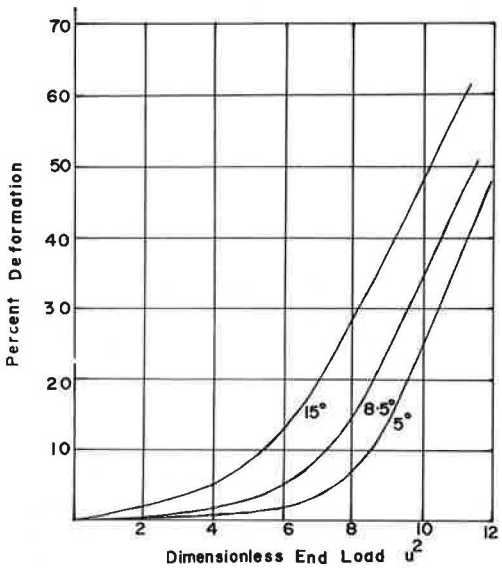

Figure 4. Dimensionless force u^2 for some values of the configuration angle α.

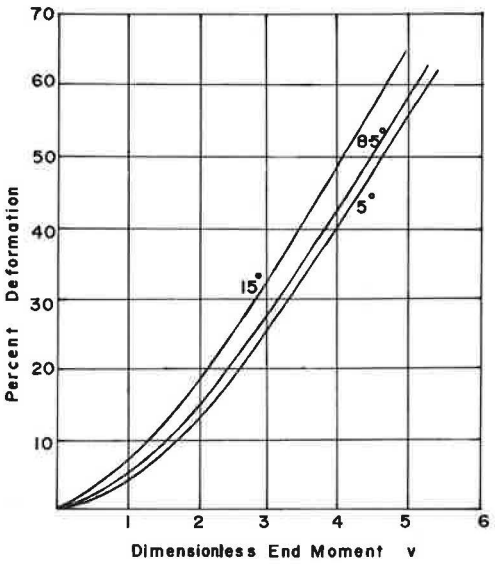

Figure 5. Dimensionless end moment v for some values of the configuration angle α.

minated when the deflection exceeds a certain predetermined value, say 80 percent. Some sample values of computer work for a configuration angle $\alpha = 8.5$ deg are given in Table 2. The numerical integration leading to these tabulated values was performed with Simpson's rule (12) by dividing the interval from ϕ_0 to $\pi/2$ into 1,000 equal steps. The error of numerical integration in these values is of the order of ±1 in the fourth significant digit. The dimensionless results for this and some other values of angle α are shown in Figures 4 and 5. Such plots are quite adequate for practical purposes, as the values of Δ and v for given u, or the values of u and v for given Δ, can be easily read off from these characteristic curves.

PREDICTION AND DISCUSSION

The results presented in the preceding section can be used to predict the actual load deflection curve for a sample that conforms with the structural assumptions made in the analysis. The sample shown in Figure 1 agrees very closely in geometry with one of the samples received for our experiments. The average values of the parameters t, ℓ, and α are 0.064 in., 0.372 in., and 8.5 deg respectively. The elastic moduli of the material of this sample are given as properties of material A in Table 1. In the analysis, the choice of the reference modulus of elasticity was left open. If we choose the modulus of elasticity in tension, E_T, as the reference elastic constant, the corresponding modified moment of inertia, I, per inch in the length of a web member is given by

$$I = (\beta^2 t^3)/[3(1 + \beta)^2] \tag{21}$$

where

$$\beta = \sqrt{E_c/E_T} \tag{22}$$

Hence, from Eq. 10 the load per inch in the length of the web member is given by

$$P = (E_T \beta^2 t^3 u^2)/[3\ell^2 (1 + \beta)^2] \tag{23}$$

For the numerical values of E_T, t, ℓ, and so on, referred to earlier in this section, Eq. 23 reduces to the form

$$P = 0.1023u^2 \text{ lb/in.} \tag{24}$$

The dimensionless load deflection curve for $\alpha = 8.5$ deg, shown in Figure 4, gives the value of u^2 for any chosen percentage deformation. When this value of u^2 is used in Eq. 24, the value of P obtained represents the end load, in pounds per inch in the length of the web member, required to produce the same value of percentage deformation. Because the sample consists of 3 web members, the load required to produce the same deformation in the sample is 3 times the value given by Eq. 24. Then, the predicted load deflection curve at room temperature is easily constructed as follows: From the curve shown in Figure 4, for angle $\alpha = 8.5$ deg, read off the value of u^2 for a selected percentage deformation, and then multiply this value by 0.307 to obtain the value of load per inch in the length of the sample for the same deformation. The predicted load deflection curve shown in Figure 6 was constructed in this manner.

The research currently in progress involves a substantial amount of experimental work. The experiments of interest in the present context are those dealing with load deflection curves, particularly those for the sample for which the theoretical prediction is shown in Figure 6. The average of two most reliable experiments out of three performed at room temperature is shown in the same figure for the purpose of comparison.

In comparing the theoretical prediction and the experimental results shown in Figure 6, it is important to take several factors into account. The theoretical prediction is made by using the average dimensions. The approximate variations in the quantities t, ℓ, and α are ±10 percent, ±5 percent and ±0.5 deg respectively. When these factors are taken into account, the theoretical prediction gives a satisfactory estimate of the actual load deflection curve, as can be seen from the closeness of the 2 curves. It was pointed out earlier that the samples are supplied in the form of coils of tubelike structure. Consequently, the side walls of the samples tested, instead of being perfect planes, are slightly curved. This fact is perhaps responsible for the sharper rise in the experimental curves in the early stages of deformation. At about 60 percent deformation, the sample becomes more like a solid mass of neoprene and does not behave like a structure. This is seen in the sharp increases in load with small increases in the deformation. The theoretical prediction, of course, does not apply to this latter situation.

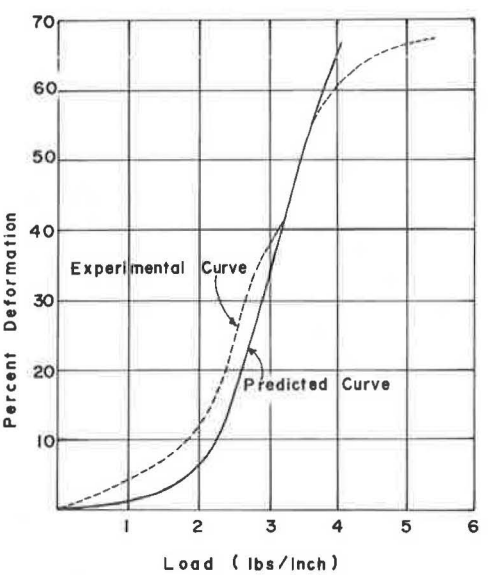

Figure 6. Predicted and experimental load deflection curves.

Although the analysis in this case gives a reasonably good estimate of the load deflection behavior, it can be further improved by taking into account the nonlinearity of the stress-strain relationship and the viscoelastic effects. The lack of sufficient information in these respects, especially for the material of an actual sample, suggests the need for more detailed experimental research in basic material properties.

The theoretical study, once the required values of the numerical constants have been ascertained, enables us to predict the maximum stresses. These occur in the web members and are evaluated from the following expressions:

$$\sigma_c(\max) = [(\lambda\beta^2 E_T)/(1+\beta)] \left(v + \{(\lambda \cos\alpha u^2)/[3(1+\beta)]\}\right) \tag{25}$$

$$\sigma_T(\max) = [\lambda\beta E_T/(1+\beta)]\left(v - \{(\lambda\beta\cos\alpha u^2)/[3(1+\beta)]\}\right) \quad (26)$$

$$\tau_{max} = \{(\lambda^2\beta^2 E_T)/[2(1+\beta)^2]\}\sqrt{u^4\sin^2\alpha + u^2v^2\cos\alpha - (v^4/4)};\ \gamma \le 90 \text{ deg} \quad (27)$$

or

$$\tau_{max} = (\lambda^2\beta^2 E_T u^2)/[2(1+\beta)^2];\ \gamma \ge 90 \text{ deg} \quad (28)$$

where

$$\lambda = t/\ell \quad (29)$$

E_T in these equations refers to the modulus of elasticity in tension; β has been defined in Eq. 22. Equations 25 and 26 refer respectively to the maximum compressive and tensile stresses. These maximum stresses occur in the web member at sections A, B, and C (Fig. 2). If the end moment v exceeds $3(1+\beta)/(\lambda\beta)$, the maximum tensile stress will occur at cross sections different from those mentioned. In practical situations, v is unlikely to exceed this value within the range for which the theoretical prediction is valid. The maximum shear stress occurs at the inflection point and is given by Eq. 27, provided the angle at inflection point is less than or equal to 90 deg. If the angle at inflection point is greater than 90 deg, the maximum shear stress given by Eq. 28 occurs at points where the neutral axis makes an angle of 90 deg with the horizontal axis.

The plots of maximum tensile and compressive stresses are shown in Figure 7. The maximum shear stress is shown in Figure 8. The shear stresses, for the example considered, are quite low, justifying the assumption made at the outset that shear deformations may be nelegected. An interesting feature is the closeness between the maximum compressive and tensile stresses, as shown in Figure 7. The near closeness of these curves is a peculiarity of this particular sample. The value of E_T for this sample is substantially larger than that of E_C. This means that the tensile stress induced by bending alone is larger than the compressive stress. When a uniform direct compressive stress due to the axial force is added to these stresses, the resulting effect is a reduction in the tensile stress and an increase in the compressive stress. The net effect is a near equalization of the 2 stresses. The situation would be much different if

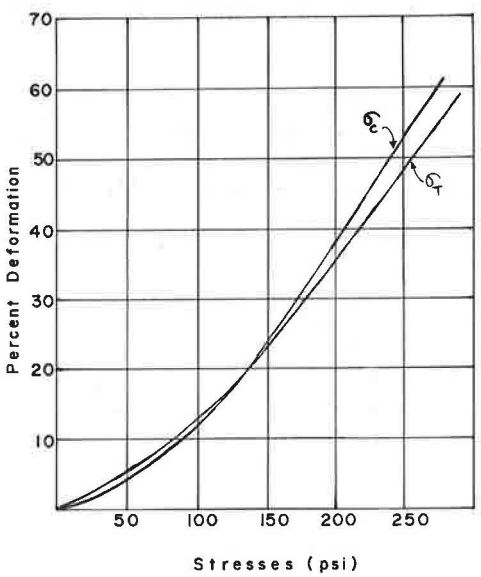

Figure 7. Predicted maximum tensile and compressive stresses.

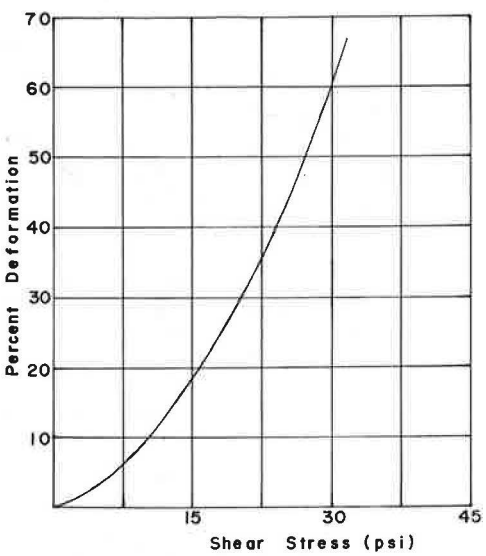

Figure 8. Predicted maximum shear stress.

this sample were made from material B or material C (Table 1). Then the compressive stress would be significantly larger.

CONCLUDING REMARKS

The theoretical technique presented here, simple as it is, gives a good estimate of the actual short time load deflection characteristics of elastomeric seals. Furthermore, it also enables prediction of maximum tensile, compressive, and shear stresses, which are of value to the designer. The dimensionless approach makes the results quite general in application and may be used to study other aspects of the performance of elastomeric seals. Specifically, one can study the effects of changes in material properties and the changes in section geometry on the stresses and stiffness of the sample. The author is currently investigating this aspect of the problem. The study may lead to some of the criteria that may be useful in producing the best design.

It is important to note that the analysis assumes linear stress-strain relationship and a typical geometry that consists of V-shaped web members. Sections with X-shaped web members, another typical arrangement, can be studied by using the same technique, but additional conditions must be incorporated in the analysis. Further refinements of the technique can be made by using nonlinear stress-strain relationship and including the fact of viscoelastic behavior in the study. Such refinements will indeed complicate an already nonlinear problem. At present, it seems that more experimental work is necessary to assess the basic properties of actual seal materials. A knowledge of these properties would be useful in making theoretical predictions regarding the short-time and long-time performance of the elastomeric seals.

ACKNOWLEDGMENTS

The author wishes to thank George Jones and Dale Peterson of the Utah State Department of Highways for the information given in Table 1. Thanks are also due to Jamie Dorman, a senior student at the University of Utah, for his efforts in the experimental part of the project. Special thanks are extended to Mrs. Merle Bryner for typing this manuscript.

This research was sponsored by American Association of State Highway Officials, in cooperation with the Federal Highway Administration, and was conducted in the National Cooperative Highway Research Program administered by the Highway Research Board. The opinions and conclusions expressed or implied in this paper are those of the author and not necessarily those of the sponsoring agencies.

REFERENCES

1. Tons, E. A Theoretical Approach to Design of a Road Joint Seal. HRB Bull. 229, 1959, pp. 20-53.
2. Cook, J. P. A Study of Polysulfide Sealants for Joints in Bridges. Highway Research Record 80, 1965, pp. 11-35.
3. Cook, J. P., and Lewis, R. M. Evaluation of Pavement Joint and Crack Sealing Materials and Practices. NCHRP Rept. 38, 1967.
4. Hiss, J. G. F., Jr., Lambert, J. R., and McCarty, W. M. Joint Seal Materials: Final Report. Bureau of Physical Research, New York State Department of Transportation, Albany, Res. Rept. 68-6, Dec. 1968.
5. Treloar, L. R. G. The Physics of Rubber Elasticity. Oxford Univ. Press, 1958.
6. Tobolsky, A. V. Properties and Structures of Polymers. John Wiley and Sons, 1967.
7. Flory, P. J. Principles of Polymer Chemistry. Cornell Univ. Press, Ithaca, New York, 1967.
8. Flügge, W. Viscoelasticity. Blaisdell Publishing Co., 1967.
9. Love, A. E. H. A Treatise on the Mathematical Theory of Elasticity. Dover Publications, New York, 1944.
10. Timoshenko, S. P., and Gere, J. M. Theory of Elastic Stability. McGraw-Hill, 1961.
11. Flügge, W., ed. Handbook of Engineering Mechanics. McGraw-Hill, 1962.
12. Hildebrand, F. B. Introduction to Numerical Analysis. McGraw-Hill, 1956.